

Journal of Materials Chemistry A

Accepted Manuscript



This is an *Accepted Manuscript*, which has been through the Royal Society of Chemistry peer review process and has been accepted for publication.

Accepted Manuscripts are published online shortly after acceptance, before technical editing, formatting and proof reading. Using this free service, authors can make their results available to the community, in citable form, before we publish the edited article. We will replace this *Accepted Manuscript* with the edited and formatted *Advance Article* as soon as it is available.

You can find more information about *Accepted Manuscripts* in the [Information for Authors](#).

Please note that technical editing may introduce minor changes to the text and/or graphics, which may alter content. The journal's standard [Terms & Conditions](#) and the [Ethical guidelines](#) still apply. In no event shall the Royal Society of Chemistry be held responsible for any errors or omissions in this *Accepted Manuscript* or any consequences arising from the use of any information it contains.

Cite this: DOI: 10.1039/c0xx00000x

www.rsc.org/xxxxxx

Full paper

Further improvement of battery performance via charge transfer enhanced by solution-based antimony doping into tin dioxide nanofibers

Yong Seok Kim^a, Won Bae Kim^b and Yong Lak Joo^{*a}

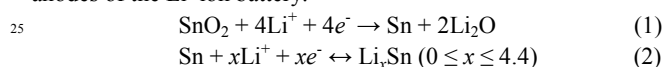
Received (in XXX, XXX) Xth XXXXXXXXX 20XX, Accepted Xth XXXXXXXXX 20XX

DOI: 10.1039/b000000x

We synthesized antimony (Sb)-doped tin dioxide (SnO₂) nanofibers by the one-pot solution doping process in electrospinning, and demonstrated that the electrical and lithium (Li)-ion conductivities of SnO₂ nanofibers can substantially be increased by such a facile doping process. Owing to improved conductivities, our Sb-doped SnO₂ nanofibers exhibited much facilitated charge transport features in battery anodes. The current study on the effect of dopant concentration revealed that 10 at.% doping represented the optimized electrical and Li-ions conductivities from current-voltage characteristics and Nyquist plots. The Sb-doped SnO₂ nanofibers retained over 95% Coulombic efficiency by all variable current rates from a low current rate of 100 mA/g to a high current rate of 1,000 mA/g, while pure SnO₂ nanofibers had lower Coulombic efficiency values around 85% at the low current rate of 100 mA/g. Especially, the doped nanofibers showed a much more stable capacity retention during 100 cycles than undoped SnO₂ nanofibers. We herein determined that the increase in charge transport features by the facile solution doping can directly lead to the improved performance of Li-ion batteries with one-dimensional nanofiber electrodes.

Introduction

Tin dioxide (SnO₂) is a promising candidate for anode electrodes of lithium (Li)-ion batteries because it exhibits a much higher theoretical capacity of 783 mAh/g than graphite (372 mAh/g).^[1] For SnO₂ electrodes, the following reactions occur in anodes of the Li-ion battery.^[1,2]



Initially, the SnO₂ is reduced into the metal Sn by lithium ions as seen in the reaction (1), and then the Sn can react with Li⁺ for the lithiation process in the reaction (2). However, it has not been widely utilized owing to a severe volume expansion of 358% as well as its poor charge transport features by the lack of charge carriers.^[3,4] In order to solve these issues, a variety of nanomaterials have been reported for a decade. For examples, one-dimensional (1-D) nanomaterials like nanowires are one of good structures not only to mitigate volume expansion but also to provide effective charge pathways.^[5,6] Also, hollow nanoparticles or porous nanotubes possess high surface areas to react with Li-ions,^[7,8] and carbon composites with SnO₂ are an efficient approach to supplement tin dioxide electrodes.^[9]

Facilitating charge transport features for SnO₂ anode electrodes is one of most critical factors to improve their battery performance, since the charges such as electrons or Li-ions should be smoothly transferred into electrodes without any loss. However, pure SnO₂ nanomaterials are still known for the poor electrical and electronic conductivities by wide energy bandgap of ca. 3.6 eV. To increase the conductivity, the doping has been

done by extrinsic *n*-type dopants (e.g., antimony, niobium or tantalum). Because antimony (Sb) is shown to be the best dopant for the enhanced electrical conductivity, Wang group examined such *n*-type dopants to promote the electrical conductivity of a SnO₂ film for transparent conducting electrodes.^[10] However, the doping under vacuum is complicated and expensive.

In the present study, pure SnO₂ nanofibers (NFs) were doped with antimony via the one-pot solution doping process in electrospinning, a very convenient and cost-effective approach. Until now, most of researchers have used expensive, high vacuum systems to dope some dopants into SnO₂ materials. For examples, Hong *et al.* reported a vapor-liquid-solid method for making Sb:SnO₂ nanoarchitectures,^[11] and thermal evaporation was used to prepare 1-D Sb-doped SnO₂ nanowires by Wang or Shih groups.^[12,13] Being able to electrospin various ratios of nominal Sn and Sb atomic percentage (at.%) from 100:0 to 85:15 in alcohol in the current approach allows us to determine the optimized electrical and Li-ion conductivities of the resulting Sb-doped SnO₂ nanofibers. Since the 10 at.% doping represented the best electrical conductivity from the *I-V* characterization, the Sb-doped SnO₂ NFs demonstrated outstanding transport features of charges (e.g., electrons or Li-ions), leading to remarkably improved battery performances such as not only discharge/charge capacity and cycle life but also Coulombic efficiency at low current rates. To best of our knowledge, there are no reports to elucidate the effects of the charge transport through the solution-based doping process for the improved performance of Li-ion batteries with 1-D nanofiber electrodes.

Experimental

Synthesis and characterization of Sb-doped SnO₂ nanofibers

In order to prepare Sb-doped SnO₂ nanofibers, the one-pot electrospinning method were used in the current study. The SnCl₂·2H₂O precursor was mixed with poly(vinyl pyrrolidone) (PVP, Mw = 1,300,000 g/mol) dissolved in methanol for pure SnO₂ nanofibers, and the precursor of SbCl₃·2H₂O was added into the solution with variable nominal atomic ratios from 100:0 to 85:15 of Sn:Sb for Sb-doped SnO₂ nanofibers. All chemicals were used as received from Sigma-Aldrich Co. without further purification. The prepared solutions loaded in a syringe were ejected at a rate of 0.01 ml/min by a syringe pump toward a vertically-placed aluminium foil collector that was 10 cm away from the needle of the syringe. As soon as a high voltage of 9.5 kV was applied to the syringe needle, the Sn and Sb precursors/PVP nanofibers were electrospun and collected on the collector. As-spun nanofibers were calcined at 600 °C for 6 h in air to remove the organic residue and produce pure SnO₂ and Sb-doped SnO₂ nanofibers. This calcination temperature was referred from valuable literatures to obtain good electrical conductivity by antimony doping.^[10] The microstructural properties of Sb-doped SnO₂ nanofibers were characterized by scanning electron microscope (SEM, LEO 1550), transmission electron microscope (TEM, FEI F20 TECNAI), X-ray diffraction (XRD, Rigaku) with a Cu K α source (λ = 1.5405 Å) and X-ray photoelectron spectroscopy (XPS, VG Multilab 2000). To examine the electrical conductivity of pure SnO₂ and Sb-doped SnO₂ nanofibers, NFs were dispersed individually in isopropyl alcohol by sonication and then dropped on a silicon wafer with the SiO₂ thickness of 100 nm. The silicon wafer is made from a highly doped *p*-type silicon, which can be used as a back gate electrode. The metal electrodes consisting of Ti (30 nm)/Au (50 nm) were deposited by an electron beam evaporator and defined as source and drain electrodes. The electronic properties of the NFs were measured using a semiconductor parameter analyzer (Agilent B-1500) at room temperature.

Battery fabrication and electrochemical measurements by using Sb-doped SnO₂ nanofibers

All pure SnO₂ and Sb-doped SnO₂ nanofibers were used as Li-ion battery negative electrodes. To fabricate battery cells using these nanofibers, Super P (from Timcal) and polyacrylic acid (Mw = 300,000) were blended with the nanofibers by 20:20:60 wt% in 1-Methyl-2-pyrrolidinone (NMP, Aldrich) to produce homogenous slurries. The prepared slurries on copper current collectors were dried in a vacuum oven at 80 °C to evaporate the NMP solvent for working electrodes in half battery cells. Li metal was used as a counter electrode, and a commercial polyethylene membrane was inserted as a separator between a working electrode and a counter electrode. The half battery cells were assembled in an Ar-filled glove box with using the home-made electrolyte composed of 1 M LiPF₆ in a solution of fluoroethylene carbonate and dimethyl carbonate (50:50 w/w). The cells using our nanofibers were measured by electrochemical impedance spectroscopy (PARSTAT 4000, Princeton Applied Research) and cyclic voltammetry (BST8-STAT, MTI) to

investigate their electrochemical properties such as activities and charge transport features. Galvanostatic charge/discharge tests of the battery cells were performed under a cut off voltage window from 0.005 to 2.0 V versus Li/Li⁺ by using charge/discharge 60 cyclers (from MTI).

Results and Discussion

In order to determine the optimized concentration of Sb doping into tin dioxide NFs, the nominal atomic percentages of antimony are changed from 0 to 15 at.% by controlling the amount of antimony precursor in electrospinning solutions. The detail experiment to fabricate electrospun Sb-doped SnO₂ NFs was written in our previous publications.^[14,15] We took energy dispersive X-ray analysis to confirm actual Sb doping percentages and summarized them in Table R1. Even though they have some errors within ± 2.0 at.%, the actual doping ratios are consistently getting increased by increasing nominal doping concentrations. As shown in photographs of Figure S1a and b, pure SnO₂ NFs exhibit white color and Sb-doped SnO₂ NFs appear blue, which means that antimony is doped within tin dioxide NFs well. Both nanofibers also have one-dimensional structures with very high aspect ratios as seen in SEM image of Figure S1c, and d. They have enough surface areas (undoped SnO₂ NFs: 29.35 m²/g, Sb-doped SnO₂ NFs: 15.97 m²/g measured by Brunauer-Emmett-Teller analyzer using nitrogen gas) to be used in Li-ion battery applications. Figure 1 shows TEM images of Sb-doped SnO₂ NFs with variable antimony doping ratios of 0, 5, 10 and 15 at.%. While pure SnO₂ NFs are composed of large nanocrystals with around 20~40 nm to coordinate 1-D nanostructures in the TEM image of Figure 1a, the crystals in Sb-doped SnO₂ NFs become smaller into under 20 nm from antimony doping as shown in Figure 1b and c of 5 at.% and 10 at.%, respectively. However, when the doping ratio is increased into 15 at.%, we again observe a few of large crystals in Sb-doped SnO₂ NFs, compared to 5 at.% or 10 at.%. The effect of the doping ratio on crystal sizes was also investigated through X-ray diffraction measurements in Figure 1e. The XRD patterns for pure SnO₂ and Sb-doped SnO₂ NFs correspond to JCPDS #41-1445 of the Cassiterite structure. There are no any additional peaks such as Sb₂O₃ or Sb₂O₅ by antimony doping; therefore, the antimony should substitute tin atoms to be doped.^[10,16,17] As seen in the patterns, while pure SnO₂ nanofibers show strong crystal diffraction peaks with narrow width, the Sb-doped SnO₂ NFs with 5 at.% and 10 at.% exhibit poor crystalline structures. Interestingly, the 15 at.% concentration shows stronger crystal diffraction peaks than other doping ratios again. This may suggest that SnO₂ crystals are segregated by antimony doping when the excessive Sb doping concentration was used to 15 at.%. Such a phenomenon also was observed in the selected area electron diffraction patterns in Figure S2. While low antimony doping concentrations exhibit diffused rings, which reflect the poor crystallinity, 20 at.% showed discrete white spots similar to pure SnO₂ NFs. By using energy dispersive X-ray spectrometry from TEM in Figure S2f, we confirmed that antimony atoms are well-distributed within the Sb-doped SnO₂ nanofibers to be doped. The XRD pattern of 20 at.% doping has the more increased peak

intensity and narrowed width than 15 at.% in Figure S3a. To examine the doping effect in tin dioxide nanofibers more, X-ray photoelectron analyses were performed as displayed in Figure 1f. In all SnO₂-based nanofibers, the Sn3d peaks are composed of Sn3d_{5/2} and Sn3d_{3/2} which ascribe Sn²⁺ and Sn⁴⁺ bonding states. By increasing the antimony doping ratio, both Sn3d peaks of Sb-doped SnO₂ NFs are slightly getting shifted to higher binding energy, compared with those of pure SnO₂ nanofibers. Furthermore, 20 at.% antimony doping showed a much higher binding energy of 486.9 eV for Sn3d_{5/2} in Figure S3b, which is a reliable evidence to confirm the antimony doping into tin dioxide structure.^[10] Also, the transmittance properties of our nanofibers were obtained by UV-visible spectroscopy to probe the nature of antimony doping in Figure S4. When the doping concentrations are getting increased, their transmittance properties are worsened gradually by excessive antimony.

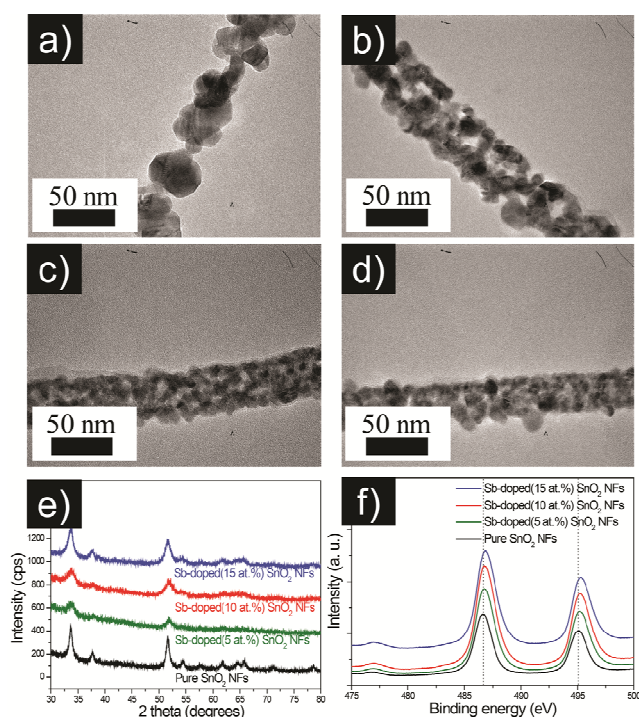


Figure 1. TEM images of (a) pure SnO₂ nanofibers and Sb-doped SnO₂ nanofibers with variable doping ratios with (b) 5 at.%, (c) 10 at.% and (d) 15 at.%; (e) x-ray patterns and (f) x-ray photoelectron Sn3d spectra of Sb-doped SnO₂ nanofibers with variable doping atomic ratios.

For investigating the electrical conductivity of pure SnO₂ and Sb-doped SnO₂ nanofibers with variable doping ratios, nanofibers were dispersed in isopropyl alcohol by sonication and then dropped on a silicon wafer with a SiO₂ thickness of 100 nm. Figure 2a presents the *I-V* characteristics of the nanofibers between source and drain electrodes. Pure SnO₂ nanofibers showed much low current, similar to a kind of insulators. The *I-V* curves of Sb-doped SnO₂ nanofibers represent good Ohmic contact features between the nanofibers and the metal electrodes. Among variable Sb doping concentrations of 5 at.%, 10 at.% and 15 at.%, the 5 at.% has a bit higher current than the pure SnO₂ NFs, and the 10 at.% especially exhibits the highest current value during voltage sweep from -1 to 1 V. In the case of 15 at.%, the

current is again decreased because the excess Sb doping concentration made phase segregation as mentioned in TEM and XRD sections. We also could not obtain any *I-V* characteristic from 20 at.% doping. The electrode distances between source and drain were changed from 10 to 40 μm to check out the *I-V* characteristic of Sb-doped SnO₂ nanofibers. The currents are typically getting decreased by the distance as seen in Figure 2b. To elucidate the improvement of Li-ions conductivity for Sb-doped SnO₂ nanofibers, we composed a three electrode cell as described in Figure 2c.^[18] The working electrode was LiCoO₂ and Li metal chip was as a counter electrode. Our Sb-doped SnO₂ nanofibers were loaded on a copper film for a reference electrode. All electrodes were sandwiched together within two stainless steel jackets and separators are able to avoid meeting each electrode directly. Because Li-ions are diffused from the working electrode to the reference electrode, we can measure the transport features of Li-ions of our nanofibers from the semicircle diameters of Nyquist plots. In particular, the 10 at.% doping has the smallest charge transport resistance among all nanofibers; note that the optimized doping concentration is able to improve the conductivity of lithium ions as well as electrical conductivity. However, the 5 at.% exhibited a much increased charge transport resistance compared with 10 at.% and even pure SnO₂ NFs. This may imply that the lack of doping could lead to the side effect for Li-ion transport.

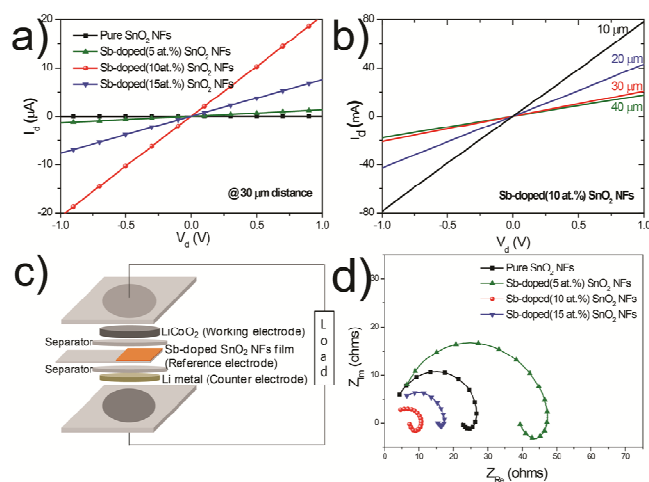


Figure 2. *I-V* curves of Sb-doped SnO₂ nanofibers with (a) variable doping atomic ratios and (b) variable electrode distances for Sb-doped (10 at.%) SnO₂ nanofibers; (c) Cell schematic to characterize Li-ion conductivity and (d) Nyquist plots of pure SnO₂ nanofibers and Sb-doped SnO₂ nanofibers with variable doping atomic ratios.

In Figure 3, the half battery cell using tin dioxide-based nanofibers were fabricated by composing of pure SnO₂ or Sb-doped SnO₂ NFs (as working electrode)/polyethylene separator/Li metal (as counter electrode). Before Li-ion battery performance tests, the electrochemical properties were investigated by cyclic voltammetry for the activity and electrochemical impedance spectroscopy for transport features of charges like electrons and Li-ions. All Sb-doped SnO₂ NFs with different doping atomic ratios possess much reduced charge transport resistances compared with pure SnO₂ NFs, as seen in the Nyquist plots of

Figure 3a. The 5 at.% doping has a decreased charge transport resistance (R_{ct}) value of 200 Ω , while the pure SnO₂ NFs have a R_{ct} value of 275 Ω . First of all, the 10 at.% doping which showed the best electrical and Li-ion conductivities displayed a much decreased R_{ct} value of 90 Ω . Again, the R_{ct} of 15 at.% is increased to 170 Ω , same to the results of electrical and Li-ion conductivities. From the results, we confirmed that the solution-based antimony doping into tin dioxide nanofibers must be valid to improve charge transport properties of the battery anodes. As seen in the Nyquist plots of Figure 3b, the facilitated charge transport features of Sb-doped SnO₂ NFs are still effective when the battery cells were measured by impedance tests after lithiation process. Because the Li-ions were already formed for LiSn compounds in the electrodes, the behaviours of mass diffusion limitation in low frequency were not observed any more. The order of charge transport resistances is similar to the results obtained from fresh battery cells as pure SnO₂ NFs > 5 at.% > 15 at.% > 10 at.% antimony doping. Moreover, only 10 at.% represents the reduced polarization resistance at a high frequency region, different from other nanofibers. To analyze the activity of pure SnO₂ NFs and Sb-doped SnO₂ NFs with variable doping ratios, the cyclic voltammetry tests were carried out as shown in Figure 3. The pure SnO₂ NFs show two lithiation peaks at 0.55 and 1.25 V vs. Li/Li⁺ and two delithiation peaks at 0.75 and 0.05 V vs. Li/Li⁺ in the initial cycle of Figure 3a. Interestingly, all Sb-doped SnO₂ NFs have a slightly shifted lithiation peak to 0.5 V vs. Li/Li⁺; note that the Sb-doped SnO₂ NFs increase electrical or electronic conductivity, compared to pure SnO₂ NFs.^[19] While the 5 and 15 at.% doping ratios exhibit similar current densities to pure SnO₂ NFs, the 10 at.% showed a much decreased peak current density. It might be contributed by well-doped antimony into tin dioxide structures, leading to reducing lithiation activity of tin materials. After 10 cycles as seen in Figure 3d, even though the peak current densities for the nanofibers of pure, 5 at.% and 15 at.% doping are decreased greatly from the first cycles of them, the 10 at.% has a less reduced peak current density than others owing to well-doped antimony.

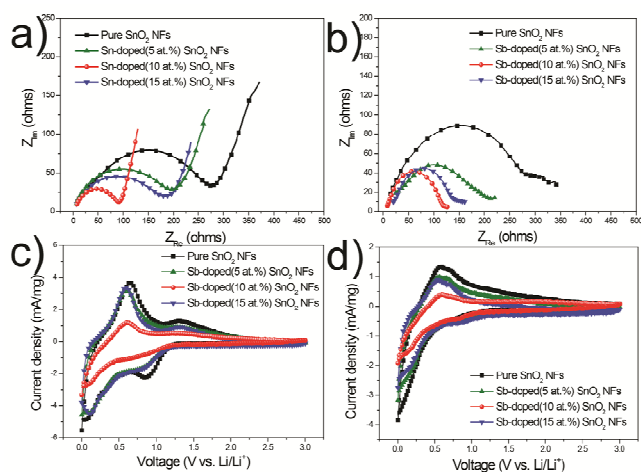


Figure 3. Nyquist plots of battery cells using Sb-doped SnO₂ nanofibers variable doping ratios (a) before and (b) after lithiation process; Cyclic voltammograms of battery cells using Sb-doped SnO₂ nanofibers variable doping ratios for (c) 1st and (d) 10th cycle.

Based on the results of previous $I-V$ characteristic and Li-ion conductivity as well as all electrochemical measurements, we believe that the 10 at.% antimony doping must be the optimum concentration for being doped into tin dioxide nanofibers.

The half cell using SnO₂ and Sb-doped SnO₂ NFs with 10 at.% doping were measured for Li-ion battery performance by galvanostatic charge/discharge process. In Figure 4a of charge/discharge curves tested at a slow current rate of 100 mA/g which mean that the electrodes are fully reacted with lithium ions, while the first discharge capacity of pure SnO₂ NFs was around 1,496 mAh/g, Sb-doped SnO₂ NFs have a decreased initial discharge capacity of 1,350 mAh/g because antimony oxide should have a smaller theoretical capacity than tin dioxide (e.g., metallic antimony theoretical capacity: 660 mAh/g).^[20] In this initial lithiation process, Sb-doped SnO₂ nanofibers would be unstably reacted with Li ions at around 0.9 V by antimony doping.^[21]

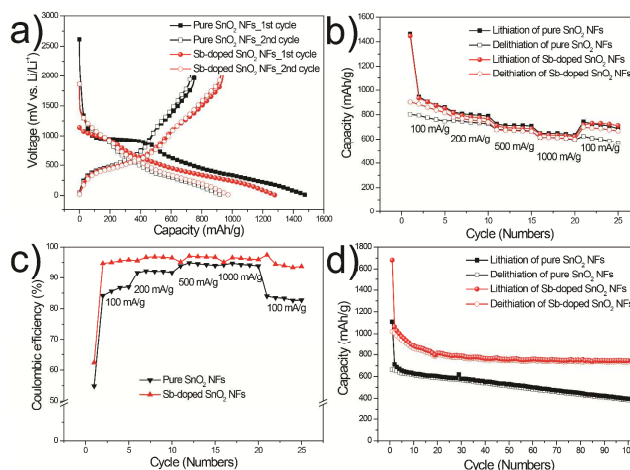
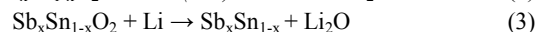
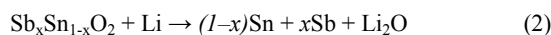


Figure 4. (a) First and second charge/discharge curves tested at 100 mA/g, (b) rate capability and (c) Coulombic efficiency with variable current rates from 100 to 1000 mA/g, and (d) long-term cycle life during 100 cycles for pure SnO₂ nanofibers and Sb-doped SnO₂ nanofibers.

Especially, the Sb-doped SnO₂ NFs exhibited a larger initial charge capacity of 980 mAh/g than pure SnO₂ NFs (720 mAh/g), and the second charge and discharge capacities of Sb-doped SnO₂ NFs become larger than those of pure SnO₂ NFs in spite of the inclusion of antimony oxide. Therefore, such increase should be attributed to facilitating transport features of charges such as electrons and lithium ions. The rate capabilities of both nanofibers were measured at variable current densities as shown in Figure 4b. Since the charge/discharge capacities of pure SnO₂ NFs and Sb-doped SnO₂ NFs are getting slightly decreased by increasing current rates from 100 to 1000 mA/g, we confirmed that both tin-based nanofibers have good rate capability features. By the way, the Sb-doped SnO₂ NFs have remarkably higher charge capacities than SnO₂ NFs at first five cycles measured by 100 mA/g current rate. After then, the difference between two nanofibers is getting smaller when the current rate is increased.

When the current rate again becomes lower to 100 mA/g, the Sb-doped SnO₂ NFs also show more charge capacities than pure SnO₂ nanofibers. From the Coulombic efficiencies up to variable current rates in Figure 4c, such behaviours are observed again. While the Sb-doped SnO₂ NFs have consistently over 95% Coulombic efficiencies with variable current rates from 100 mA/g to 1,000 mA/g, the pure SnO₂ NFs exhibit much less Coulombic efficiencies (around 85% or 90%) at slow current rates such as 100 or 200 mA/g. In Figure 4d of the long-term cycle life during 100 cycles, Sb-doped SnO₂ NFs showed much more stable without capacity fading and severe volume expansion as well as higher capacity than pure SnO₂ NFs, owing to enhancing charge conductivity from antimony doping. As seen in this result, the SEI layers formed by cycling did not decrease battery performance in high-conductive Sb-doped SnO₂ NFs anode. Finally, the morphology and electrochemical performance for the doped NFs prepared at higher temperature is shown in Figure S5. It is observed that the dope NFs prepared at 800 °C exhibit much larger crystal sizes and a slightly worse cycle life with lower capacity than those prepared at 600 °C possibly due to the increased resistivity at higher temperature.^[10]

Conclusions

In summary, we successfully doped antimony into one-dimensional SnO₂ nanofibers via the one-pot electrospinning solution process without any additional steps. Among variable doping ratios from 5 at.% to 15 at.%, the 10 at.% concentration represented the best electrical and Li-ions conductivities, and our Sb-doped SnO₂ nanofibers exhibited a much improved charge transport features in Li-ion battery anodes. The Sb-doped SnO₂ nanofibers showed that their discharge/charge capacities were increased and the long-term cycle life became much stable, compared to pure SnO₂ nanofibers. Especially, Sb-doped SnO₂ nanofibers have over 95% Coulombic efficiencies at whole variable current rates, whereas pure SnO₂ nanofibers showed poor Coulombic efficiency values below 85% at slow current rates. Such improvement of the battery performance by using Sb-doped SnO₂ nanofibers should be attributed to the facilitation of charge transport features from doping antimony. We herein demonstrated that the modification of charge transport features through the feasible solution-based doping process can apparently improve the battery anodes with the 1-D nanofibrous system.

Notes and references

- ^a School of Chemical and Biomolecular Engineering, Cornell University, Ithaca, 14853, USA. E-mail: ylj2@cornell.edu
- ^b School of Materials Science and Engineering, Gwangju Institute of Science and Technology (GIST), Gwangju, 500-712, Republic of Korea.

† Electronic Supplementary Information (ESI) available: [EDX data, photographs and SEM images, Selected electron diffraction patterns with antimony mapping image, XRD and XPS spectra, transmittance spectra of the nanofibers, and TEM image and additional cycle life]. See DOI: 10.1039/b000000x/.

- 1 J. S. Chen, X. W. Luo, *Small* **2013**, *9*, 1877–1893.

- 2 Y. Idota, T. Kubota, A. Matsufuji, Y. Maekawa, T. Miyasaka, *Science* **1997**, *276*, 1395–1397.
- 3 C. Kim, M. Noh, M. Choi, J. Cho, B. Park, *Chem. Mater.* **2005**, *17*, 3297–3301.
- 4 Q. Wan, E. Dattoli, W. Lu, *Small* **2008**, *4*, 451–454.
- 5 M. S. Park, G. X. Wang, Y. M. Kang, D. Wexlaer, S. X. Dou, H. K. Liu, *Angew Chem. Int. Ed.* **2007**, *46*, 750–753.
- 6 Y. Wang, J. Y. Lee, H. C. Zeng, *Chem. Mater.* **2005**, *17*, 3899–3903.
- 7 S. J. Ding, J. S. Chen, G. G. Qi, X. N. Duan, Z. Y. Wang, E. P. Giannelis, L. A. Archer, X. W. Lou, *J. Am. Chem. Soc.* **2011**, *133*, 21–23.
- 8 Y. Wang, H. C. Zeng, J. Y. Lee, *Adv. Mater.* **2006**, *18*, 645–649.
- 9 C. A. Bonino, L. Ji, Z. Lin, O. Toprakci, X. Zhang, S. A. Khan, *ACS Appl. Mater. Interfaces* **2011**, *3*, 2534–2542.
- 10 Y. Wang, T. Brezesinski, M. Antonietti, B. Smarsly, *ACS Nano* **2009**, *3*, 1373–1378.
- 11 S. Park, S. -D. Seo, S. Lee, S. W. Seo, K. -S. Park, C. W. Lee, D. -W. Kim, K. S. Hong, *J. Phys. Chem. C* **2012**, *116*, 21717–21726.
- 12 Q. Wan, T. H. Wang, *Chem. Commun.* **2005**, *14*, 3841–3843.
- 13 P. -S. Lee, Y. -H. Lin, Y. -S. Chang, J. -M. Wu, *Thin Solid Films* **2010**, *519*, 1749–1754.
- 14 Y. S. Kim, H. S. Jang, W. B. Kim, *J. Mater. Chem.* **2010**, *20*, 7859–7863.
- 15 Y. S. Kim, B. -K. Yu, D. -Y. Kim, W. B. Kim, *Sol. Energy Mater. Sol. Cells* **2011**, *95*, 2874–2879.
- 16 S. Park, S. -D. Seo, S. Lee, S. W. Seo, K. -S. Park, C. W. Lee, D. -W. Kim, K. S. Hong, *J. Phys. Chem. C* **2012**, *116*, 21717–21726.
- 17 J. Suffner, S. Kaserer, H. Hahn, C. Roth, F. Eittinghausen, *Adv. Energy Mater.* **2011**, *1*, 648–654.
- 18 H. -M. Cho, Y. J. Park, H. -C. Shin, *J. Electrochem. Soc.* **2010**, *157*, A8–A18.
- 19 Y. S. Kim, K. W. Kim, D. Cho, N. S. Hansen, J. Lee, Y. L. Joo, *ChemElectroChem* **2014**, *1*, 220–226.
- 20 H. Wu, Y. Cui, *Nano Today* **2012**, *7*, 414–429.
- 21 F. D. Wu, M. Wu, Y. Wang, *Electrochem. Commun.* **2011**, *13*, 433–436.

Title: Further improvement of battery performance via charge transfer enhanced by solution-based antimony doping into tin dioxide nanofibers

Authors: *Yong Soek Kim, Won Bae Kim, and Yong Lak Joo**, School of Chemical and Biomolecular Engineering, Cornell University, Ithaca, NY, 14853

Text: Enhanced charge transport by facile Sb doping to SnO₂ nanofibers leads to improved capacity and cyclability in Li-ion battery application.

